Scientific Research and Essays Vol. 7(47), pp. 4092 -4099, 3 December, 2012
Available online at http://www.academicjournals.org/SRE
DOI: 10.5897/SRE12.647
ISSN 1992-2248 ©2012 Academic Journals

Full Length Research Paper

Effects of baffles geometry on sloshing dynamics of a viscous liquid tank

Morteza Shahravi and Milad Azimi*

Space Research Center, Tehran, Iran.

Accepted 17 October, 2012

Baffles are used effectively to reduce the sloshing response of liquid in the liquid storage containers. In this paper, a brief equivalent method is proposed to model the influence of different baffle geometrical effects on liquid sloshing. It has been showed that the natural frequencies and the dynamic response of the liquid in the container are drastically changed if the free liquid surface in a cylindrical container is being covered with structural parts. The advantages of a partly covered free surface plane lies in the shifting of the natural propellant frequencies above and away from the control frequency of a space vehicle, and in the decrease of the sloshing masses participating in the dynamic motion of the system. The fundamental natural frequency of a viscous and incompressible liquid has been determined for different geometrical shape and width of an annular ring baffle attached to the tank wall. The response to translational and pitching excitation has also been evaluated and showed the shifting of the resonance margins to higher values. Simulation results showed the effectiveness of this procedure. The presented approach may be applied to the various arbitrary coverage of free liquid surface and different geometry of container.

Key words: Sloshing dynamics, incompressible liquid, translational/pitching excitation.

INTRODUCTION

With the increasing amount of liquid on board spacecraft, liquid management and its influence on the overall spacecraft dynamics is becoming increasingly important. The influence of sloshing liquid may hamper critical maneuvers in space such as the docking of liquid-cargo vehicles or the pointing of observational satellites. Several serious problems with sloshing liquid in spacecraft have been reported over the years. For example, pendulum models or spring–mass models are used to simulate liquid sloshing in many cases. This kind of equivalent mechanical model which is based on the assumption of small amplitude sloshing is originated in 1960s. These searchers and engineers such as Abramson (1996), Dodge (2000), Wang et al. (2002), Qing et al. (2011) and Ibrahim (2005) have done a lot of work through analytical derivations, numerical computations and experiments which forms a collection of representative literature. Besides, applications and studies of such models have been taken in a wide range of fields by Aliabadi et al. (2003). When a tank is partially filled with fluid, a free surface is present. Then, rigid body acceleration of the tank produces a subsequent sloshing of the fluid. During this motion, it supplies energy to sustain the sloshing thus causing violent motion in the unrestrained free surface. Depending upon the type of disturbance and container shape, the free liquid surface can experience different motions like simple planer, non-planer, rotational, irregular beating, symmetric, asymmetric, quasi-periodic and chaotic. Pal et al. (2002) and Akyildiz et al. (2006) declare that the amplitude of slosh, in general, depends upon the nature, amplitude and frequency of the tank motion, liquid-fill depth, liquid properties and tank geometry.

*Corresponding author. E-mail: milad_azimi@mecheng.iust.ac.ir. Tel: +989122481478.

Celebi et al. (2002) have simulated the problem of fluid motion in partially filled rectangular tanks using the volume of fluid formation to track the free surface. They solved the complete Navier–Stokes equation in primitive variables by the use of the finite difference approximations. A mechanical model of liquid sloshing was developed by Xu and Dai (2003) to investigate the longitudinal dynamic characteristics of partially filled liquid cargo tank vehicles during typical straight-line driving. The dynamic liquid motion is modeled by using a mechanical system that describes the behavior of the liquid motion as a linear spring–mass model augmented with an impact subsystem for longitudinal oscillations. Computer simulation of tank vehicles under rough road conditions is performed by incorporating the forces and moments caused by liquid motion into the pitch plane vehicle model. Usually, the sloshing effect is suppressed in a passive manner by introducing additional sub-structures called baffle or sloshing damper into the containers by Gedikli et al. (1999) and Modi et al. (2002). Also, Welt et al. (1992), Lee and Cho (2002) and Cho and Lee (2003) demonstrated that the shape and design concept of the sloshing damper varies depending on the sloshing motion type, the kind of external excitation and the container shape. Representative examples of the sloshing damper are annular ring baffle installed slightly below the liquid free surface, semi-spherical obstacles installed at the bottom plate of container, wedge with holes installed inclined to the flow direction. The basic concept of passive sloshing damper is to dissipate the sloshing motion energy by breaking a main sloshing flow into several weaker sub-streams.

Dynamic modeling

Figure 1 shows a schematic diagram of an equivalent dynamic model consisting of a rigid mass m_0 moving in unison with the tank, and a series of masses, m_n representing the equivalent mass of each sloshing portion. Each modal mass, m_n is restrained by a spring, K_n and a dashpot, C_n which contains viscous damping of the fluid and additional damping of the baffles. Total mass at the fluid can be considered as (Ibrahim, 2005):

$$m_F = m_0 + \sum_{n=1}^{\infty} m_n \tag{1}$$

Mass moment of inertia about the y-axis that passes through the center of mass of the solidified liquid:

$$I_f = I_0 + m_0 h_0^{\,2} + \sum_{n=1}^{\infty} m_n h_n^{\,2} \tag{2}$$

The center of mass should be preserved:

$$m_0 h_0 - \sum_{n=1}^{\infty} m_n h_n = 0 \tag{3}$$

The spring constants k_n can be determined from the definition of natural frequencies. For example, with reference to an upright cylindrical tank we have:

$$\omega_n^{\,2} = \frac{K_n}{m_n} = \left(\frac{g\xi_{1n}}{R}\right)\tanh\left(\frac{\xi_{1n} h}{R}\right) \tag{4}$$

Let x_n be the displacement of the equivalent mass relative to the container wall, x the displacement of the container, ψ the rotational motion of the container about the y-axis through the center of the equations of motion of the equivalent model may be derived using Lagrange's equation:

$$\frac{d}{d_t}\left(\frac{\partial}{\partial \dot{q}_i} L\right) - \frac{\partial}{\partial q_i} L = -\frac{\partial}{\partial \dot{q}_i} \Im + Q_i \tag{5}$$

Where Lagrangian $L = T - V$, q_i are the generalized coordinates, Q_i are the generalized forces, $\Im$ is the Rayleigh dissipation energy function, T and V are the kinetic and potential energies, respectively. The kinetic energy is:

$$T = \frac{1}{2} m_0 (\dot{X} - h_0 \dot{\psi})^2 + \frac{1}{2} I_0 \dot{\psi}^2 + \frac{1}{2} \sum_{n=1}^{\infty} m_n (\dot{X}_n + \dot{X} + h_n \dot{\psi})^2 \tag{6}$$

The potential energy is:

$$V = \frac{1}{2} g \psi^2 m_0 h_0 - \frac{1}{2} g \psi^2 \sum_{n=1}^{\infty} m_n h_n - g\psi \sum_{n=1}^{\infty} m_n X_n + \frac{1}{2} \sum_{n=1}^{\infty} K_n X_n^{\,2} \tag{7}$$

The dissipation energy is:

$$\Im = \frac{1}{2} \sum_{n=1}^{\infty} C_n \dot{X}_n^{\,2} + = \sum_{n=1}^{\infty} m_n \omega_n \zeta_n \dot{X}_n^{\,2} \tag{8}$$

The dashpot $C_n = 2 m_n \omega_n \zeta_n$ and ζ_n is the damping factor of the equivalent dashpot. The generalized coordinates, q_i and forces, Q_i are given by the following vectors:

$$\{q_i\} = \{x \;\; x_n \;\; \psi\}^T \;, \quad \{Q_i\} = \{-F_x \;\; 0 \;\; M_y\} \tag{9}$$

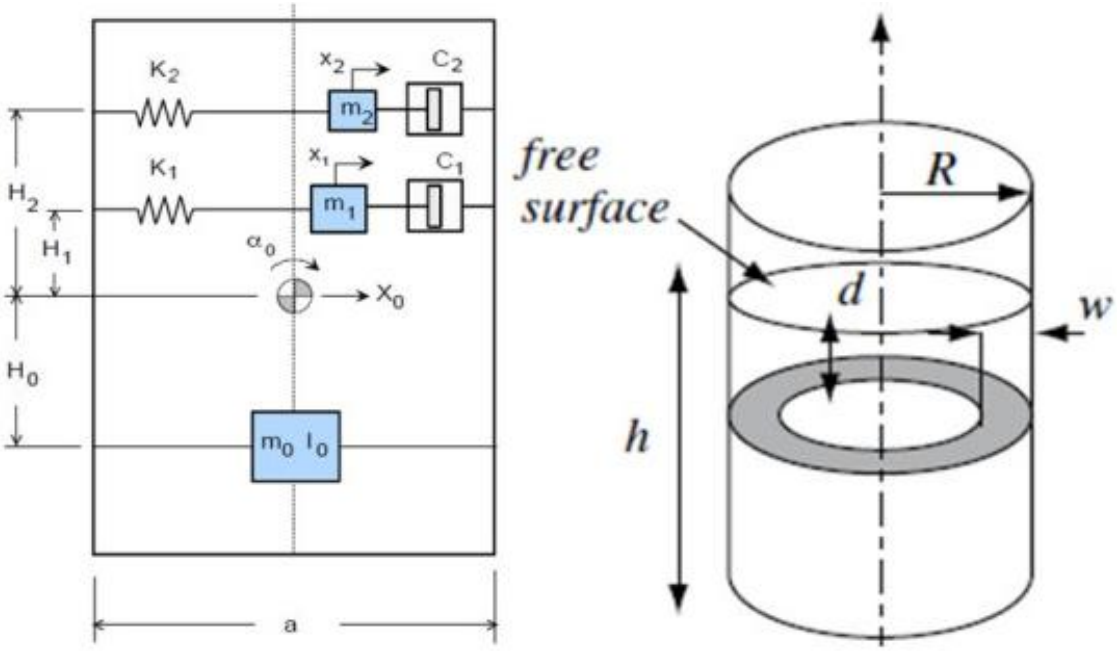

Figure 1. Viscous liquid in cylindrical tank, physical and analytical model.

Applying Lagrange's Equation 5, using expressions in Equations 6, 7, 8 and 9 gives the following equations of motion. Force equation:

$$m_0(\ddot{X} - h_0\ddot{\psi}) + \sum_{n=1}^{\infty} m_n(\ddot{X} + \ddot{X}_n + h_n\ddot{\psi}) = -F_x \quad (10)$$

Slosh equation of nth mode:

$$m_n(\ddot{X}_n + \ddot{X} + h_n\ddot{\psi}) + K_n X_n + 2m_n\omega_n\zeta_n\dot{X}_n - m_n g\psi = 0 \quad (11)$$

Moment equation:

$$I_0\ddot{\psi} - m_0h_0(\ddot{X} - h_n\ddot{\psi}) - g\sum_{n=1}^{\infty} m_n X_n + \sum_{n=1}^{\infty} m_n X_n\,(\ddot{X}_n + \ddot{X} + h_n\ddot{\psi}) = M_y \quad (12)$$

For pure translational excitation, $x(t) = X_0\,Sin\Omega t$, $\psi = 0$ which X_0 is the excitation amplitude and Ω, the forcing frequency, and zero damping, the slosh equation takes the form:

$$m_n\ddot{X}_n + K_n X_n = m_n X_0\Omega^2 Sin\Omega t \quad (13)$$

The steady state solution of this equation is:

$$X_n = \frac{\Omega^2}{\omega_n^2 - \Omega^2} X_0 Sin\Omega t \quad (14)$$

The force equation is:

$$F_x = -m_0\ddot{X} - \sum_{n=1}^{\infty} m_n(\ddot{X}_n + \ddot{X}) = X_0\Omega^2\,Sin\Omega t.\{m_0 + \sum_{n=1}^{\infty} m_n[\frac{\Omega^2}{\omega_n^2 - \Omega^2} + 1]\} \xrightarrow{\times m_F}$$
$$= m_F X_0\Omega^2 Sin\Omega t.\{1 + \sum_{n=1}^{\infty}\frac{m_n}{m_F}[\frac{\Omega^2}{\omega_n^2 - \Omega^2}\} \quad (15)$$

The moment equation is:

$$M_y = -m_0h_0\ddot{X} - g\sum_{n=1}^{\infty} m_n X_n + \sum_{n=1}^{\infty} m_n h_n(\ddot{X}_n + \ddot{X}) = -X_0\,\Omega^2\,Sin\Omega t.\{m_0h_0 + \sum_{n=1}^{\infty}[\frac{gm_n}{\omega_n^2 - \Omega^2}]$$
$$+ \sum_{n=1}^{\infty} m_n h_n[\frac{\Omega^2}{\omega_n^2 - \Omega^2}]\} = -X_0\,\Omega^2\,Sin\Omega t \times \{m_0h_0 + \sum_{n=1}^{\infty} m_n[X_n + \frac{g}{\omega_n^2}] + \sum_{n=1}^{\infty} m_n[X_n + \frac{g}{\omega_n^2}].[\frac{\Omega^2}{\omega_n^2 - \Omega^2}]\} \quad (16)$$

Under pitching excitation about the y-axis, $\psi(t) = \psi_0 \, Sin\Omega t$, the equations of motion are:

$$m_n \ddot{X}_n + K_n X_n = m_n (g + h_n \Omega^2) \Psi_0 \, Sin\Omega t \quad (17)$$

The steady-state response is:

$$X_n = \frac{(h_n \Omega^2 + g)}{\omega_n{}^2 - \Omega^2} \Psi_0 Sin\Omega t \quad (18)$$

The resulting force is:

$$F_x = -[m_0 h_0 \ddot{\psi} + \sum_{n=1}^{\infty} m_n (\ddot{X}_n + h_n \ddot{\psi}) = \Psi_0 \, \Omega^2 \, Sin\Omega t \times \{m_0 h_0 + \sum_{n=1}^{\infty} m_n (h_n \Omega^2 + g) \times [\frac{\omega_n{}^2}{\omega_n{}^2 - \Omega^2}]\} \quad (19)$$

The moment about the y-axis is:

$$M_y = I_0 \ddot{\psi} + m_0 h_0{}^2 \ddot{\psi} - g \sum_{n=1}^{\infty} m_n \, X_n + \sum_{n=1}^{\infty} m_n h_n (\ddot{X}_n + h_n \ddot{\psi}) = \psi_0 \, \Omega^2 \, Sin\Omega t$$
$$\times \{I_0 + m_0 h_0{}^2 + \sum_{n=1}^{\infty} m_n [h_n \Omega^2 + g]^2 [\frac{\omega_n{}^2}{\omega_n{}^2 - \Omega^2}] \quad (20)$$

The hydrodynamic force due to combined translational and pitching excitations is:

$$F_x = m_f X_0 \, \Omega^2 Sin\Omega t \, . \{1 + \sum_{n=1}^{\infty} \frac{2R\Omega^2 \tanh(\frac{\zeta_{1n} h}{R})}{\zeta_{1n} h (\zeta_{1n}{}^2 - 1)(\omega_n{}^2 - \Omega^2)}\} + m_f \psi_0 \, \Omega^2 Sin\Omega t \, . \{\sum_{n=1}^{\infty} \frac{2R\Omega^2 \tanh(\frac{\zeta_{1n} h}{R})}{\zeta_{1n} h (\zeta_{1n}{}^2 - 1)}\} \times$$
$$\frac{[\frac{h}{2} \Omega^2 (1 - (\frac{4R}{\zeta_{1n}} h)) . \tanh(\frac{\zeta_{1n} h}{R}) + g]}{(\omega_n{}^2 - \Omega^2)} \quad (21)$$

Comparing the first expression with Equation 15, and the second expression with Equation 19, the following equivalent parameters are obtained:

$$\frac{m_n}{m_F} = \frac{2R}{\zeta_{1n} h (\zeta_{1n}{}^2 - 1)} . \tanh(\frac{\zeta_{1n} h}{R}) \quad (22)$$

$$\frac{m_0}{m_f} = 1 - \sum_{n=1}^{\infty} \frac{m_n}{m_f} = 1 - \frac{2R}{\zeta_{1n} h (\zeta_{1n}{}^2 - 1)} . \tanh(\frac{\zeta_{1n} h}{R}) \quad (23)$$

$$\frac{h_n}{h} = \frac{1}{2} [1 - \frac{4R}{\zeta_{1n} h} . \tanh(\frac{\zeta_{1n} h}{2R})] \quad (24)$$

From the definition of the center of mass in Equation 3 and using relations in Equations 22, 23 and 24, one can write:

$$\frac{h_0}{h} = \frac{1}{1 - \sum_{n=1}^{\infty} \frac{2R}{\tanh(\zeta_{1n}{}^2 - 1)} \tanh(\frac{\zeta_{1n} h}{R})} \times [\frac{1}{2(\frac{h}{R})^2} - \sum_{n=1}^{\infty} \frac{\zeta_{1n} \tanh(\frac{\zeta_{1n} h}{R}) + 4 \frac{R}{h Cosh(\frac{\zeta_{1n} h}{R})}}{\zeta_{1n}{}^2 (\zeta_{1n}{}^2 - 1) \frac{h}{R}} \quad (25)$$

The pitching moment caused by sloshing hydrodynamic forces is:

$$M_y = \psi_0 \Omega^2 Sin\Omega t \times \{I_F + m_f \sum_{n=1}^{\infty} \frac{2Rh^2 \Omega^2 \tanh(\frac{\zeta_{1n} h}{R})}{\zeta_{1n} h (\zeta_{1n}{}^2 - 1)} \times \frac{[1 - (\frac{4R}{\zeta_{1n} h}) \tanh(\frac{\zeta_{1n} h}{R})]^2}{4(\omega_n{}^2 - \Omega^2)} + m_f . \sum_{n=1}^{\infty} \frac{2R \tanh(\frac{\zeta_{1n} h}{R})}{\zeta_{1n} h (\zeta_{1n}{}^2 - 1)} \times$$
$$. \left\{ \frac{(\frac{g}{\Omega})^2 + gh[1 - (\frac{4R}{\zeta_{1n} h}) \tanh(\frac{\zeta_{1n} h}{R})]}{(\omega_n{}^2 - \Omega^2)} \right\} + m_f \, X_0 \Omega^2 Sin\Omega t \sum_{n=1}^{\infty} \frac{2R \tanh(\frac{\zeta_{1n} h}{R})}{\zeta_{1n} h (\zeta_{1n}{}^2 - 1)} \} \times \left\{ \frac{g + (\frac{h\Omega^2}{2})[1 - (\frac{4R}{\zeta_{1n} h}) \tanh(\frac{\zeta_{1n} h}{R})]}{(\omega_n{}^2 - \Omega^2)} \right\} \quad (26)$$

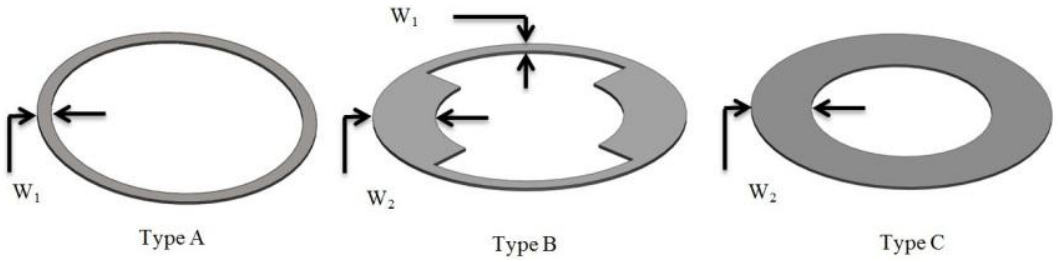

Figure 2. Different baffles geometry.

This moment is a combination of the moments due to pitching and translation which should be equivalent to the sum of Equations 16 and 20. Comparing this with Equation 26, gives:

$$I_F = I_0 + m_0 h_0^{\,2} + \sum_{n=1}^{\infty} m_n h_n^{\,2} \qquad (27)$$

$$I_F = m_f \left\{ \frac{h^2}{12} + \frac{R^2}{4} - 8R^2 \sum_{n=1}^{\infty} \frac{1 - (\frac{2R}{\zeta_{1n} h}) \tanh(\frac{\zeta_{1n} h}{2R})}{\zeta_{1n} (\zeta_{1n}^{\,2} - 1)} \right\} \qquad (28)$$

The moment I_F is the actual mass moment of inertia of the liquid about the y-axis through its center of mass.

RESULTS

An incompressible and frictionless liquid is assumed to perform ii-rotational motion in a circular cylindrical container filled to the height of $h\,(h = 1(m))$ and exhibiting a diameter of $R\,(R = 0.25(m))$. The free liquid surface is partially covered by an annular structural rigid surface mounted on the cylindrical wall (Figure 1). It may be of interest to remark that the results of the following treatment could also be used for checking numerical methods such as finite element and others, applicable to more complex geometries (Ehrlich et al., 1961; Lomen, 1995). It should also be mentioned that the liquid motion in ship-tankers, railroad and road tankers could be considerably calmed by such additional structural devices at the location of the free surface, thus resulting in an enhanced and fail-safe handling of the vehicle. For free oscillations of a liquid in a stationary tank, there is no energy input and the amplitude of successive slosh oscillations decreases because of energy dissipation. The analytical determination of damping due to baffles is not an easy task and the most effective way is to measure it experimentally.

The damping provided by a ring baffle is analyzed by analogy to the drag that a flat plate exerts on an oscillatory flow and the liquid is assumed to oscillate in the fundamental slosh mode. The damping coefficient for a ring baffle in a cylindrical case is predicted to be (Ehrlich et al., 1961):

$$\zeta = 2.83 e^{-4.6(d/R)} \left(\frac{w}{R}\left(2 - \frac{w}{R}\right)\right)^{3/2} \left(\frac{\gamma}{R}\right). \qquad (29)$$

Where w is the plate width, d distance of baffle below the free surface, γ is sloshing wave amplitude.

As depicted in Figure 2, three diverse baffles geometry with $w_1 = 0.05(m), w_2 = 0.2(m)$ are considered. The largest feasible slosh amplitude that can be assumed reasonably is $0.2R$ (unless nonlinear effects can be analyzed). Predicted and measured damping values for different baffle geometries near the liquid surface as a function of baffle submergence depth for sloshing amplitude 0.00834 are shown in Figure 3 (Abramson et al., 1960). The response of the free liquid surface to combined translational and pitching excitations with $x_0 = 100$, $\psi_0 = 50$ is presented in Figure 4 and also it depicted three different geometrical baffle type effects on displacement of 5 sloshing masses. We notice that with the increase of the baffle width, there is a much decreased displacement distribution inside the container. This does not only mean that the resonance frequency exhibits a larger value, but it also means that the sloshing mass participating in the motion is somewhat reduced. The modal analysis of the system is shown in Figure 5 and also a comparison of different sloshing masses displacement which is affected by ring baffle type C is represented in Figure 6. As we can see, the inserted baffle (Type C) in the location of quintuplicate sloshing mass, the amplitude of the sloshing is decreased.

DISCUSSION

Sloshing is the superposition of surface waves. Several forces determine the nature of these waves. When the fluid is not rotating, the relevant forces are surface tension and gravity. With rotation, the centrifugal and Coriolis forces are also present. The combined effect of

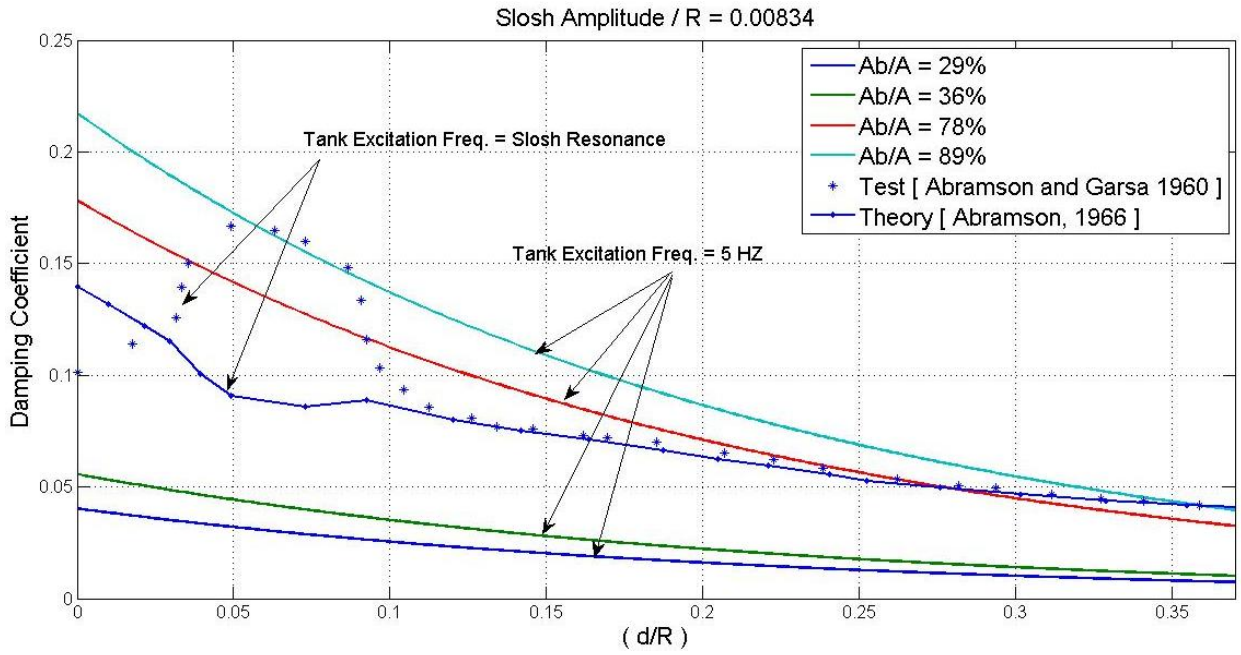

Figure 3. Comparison of ring baffle damping theory as a function of submergence depth ratio $\frac{d}{R}$, for $\frac{\gamma}{R} = 0.2$.

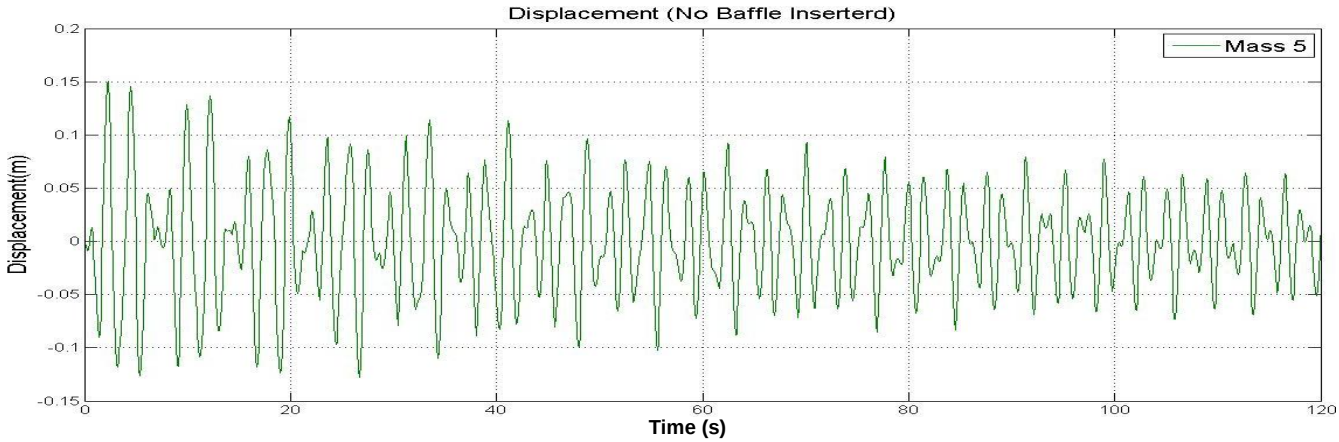

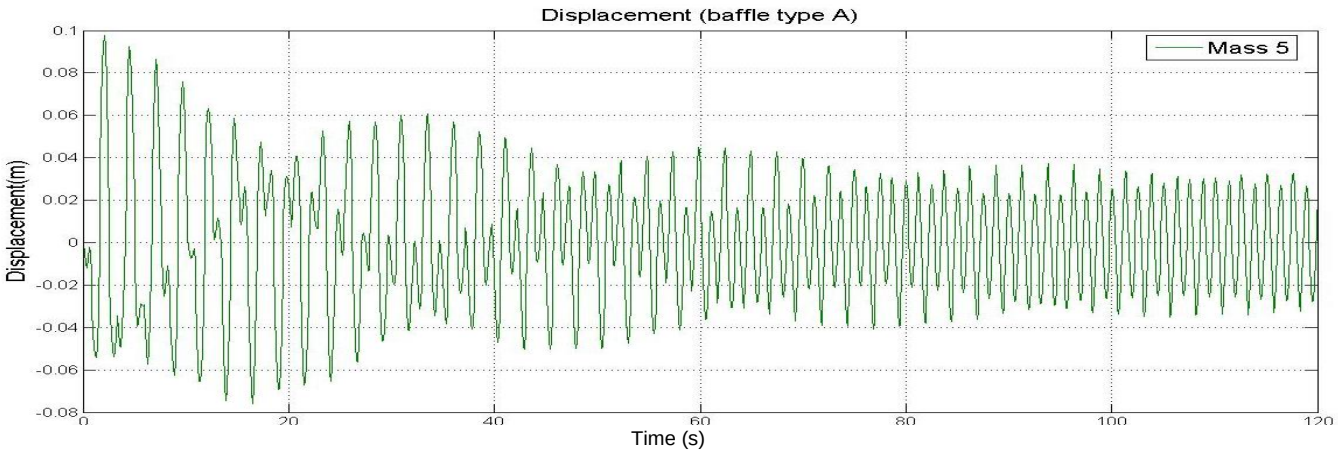

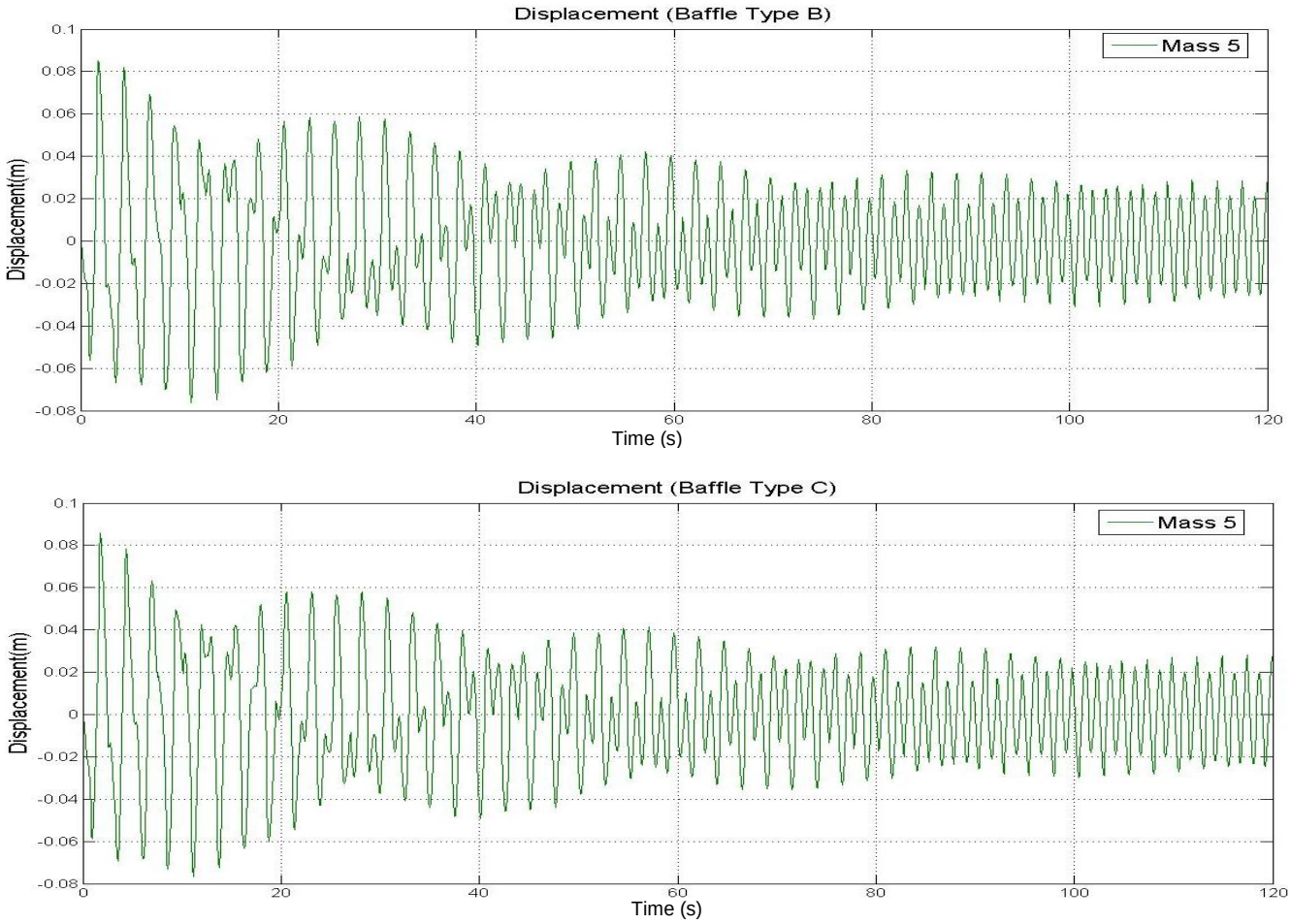

Figure 4. Comparison of different ring baffle geometry effects on dynamical behaviour of quintuplicate mass, for $\frac{\gamma}{R}=0.2$ $\frac{d}{R}=0.068$.

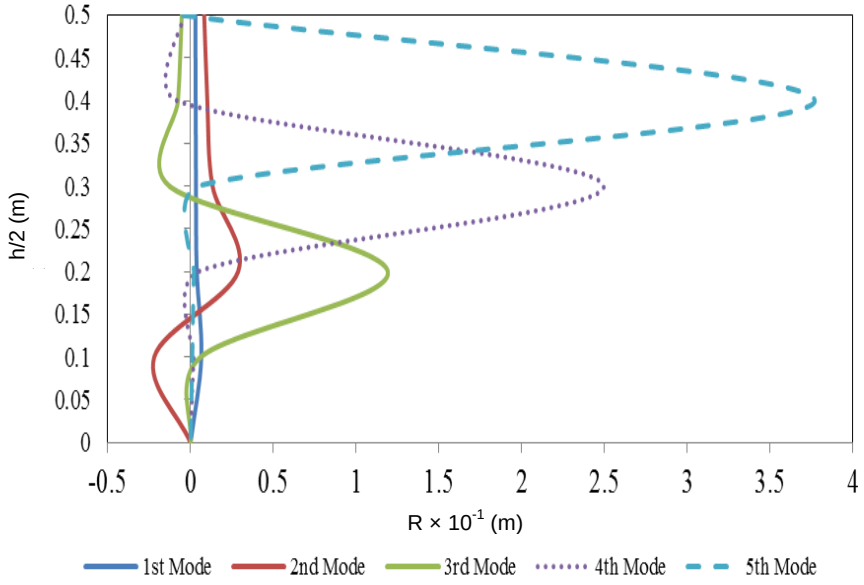

Figure 5. Vibrational modes diagram of baffled liquid tank.

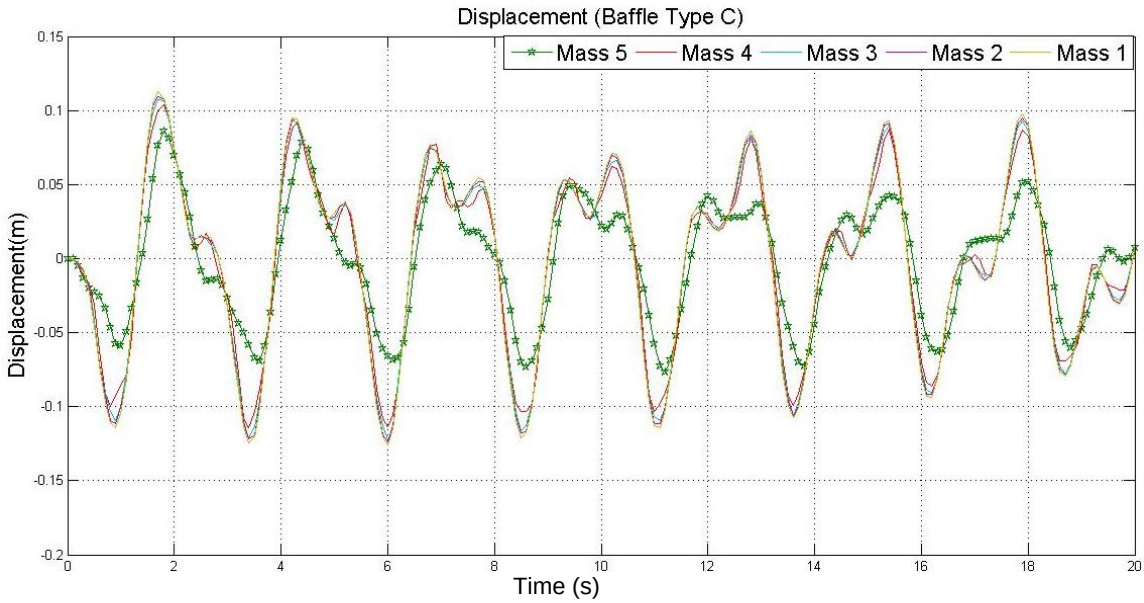

Figure 6. Dynamical behavior of baffled liquid tank.

translations and rotations of water is quite important as the water present in the tank behaves slightly compressible. Here, we notice that by merely introducing such an annular baffle, the natural frequencies may be shifted considerably to larger magnitudes and that the sloshing masses decrease, indicating a much reduced influence of the sloshing propellant upon the control and the stability of the aerospace vehicle. Also, increasing the baffle width ratio of w/d, increases the fundamental natural frequency of the propellant.

Conclusion

A dynamical model of a propellant baffled tank with multiple slosh modes has been developed. The effects of the annular baffles at the container wall in the free liquid surface have been studied quantitatively using different baffles damping theory. Changes in the natural vibrational modes and dynamical response of the tank have been shown, considering three typical baffles geometry and various depths of the submerged baffles. The sloshing amplitude of the propellant is quite changed with the increase of the baffle width w, however the natural frequencies of the tank changed drastically. The presented method may easily be applied to any structural system in the free surface plane, and maybe used for showing the adequacy of purely numerical methods such as finite element methods.

REFERENCES

Abramson HN (1996). The dynamic behaviour of liquids in moving containers, NASA SP-106.
Abramson HN, Ransleben GE (1960). Simulation of Fuel Sloshing in Missile Tanks by Use of Small Models. ARS J. 30:603-612.
Akyildiz H, Unal NE (2006).Sloshing in a three-dimensional rectangular tank: Numerical simulation and experimental validation. J. Ocean Eng. 33:2135–2149.
Aliabadi S, Johnson A, Abedi J (2003). Comparison of finite element and pendulum models for simulation of sloshing. J. Comput. Fluids 32:535–545.
Celebi MS, Akyildiz H (2002). Nonlinear modelling of liquid sloshing in a moving rectangular tank. J. Ocean Eng. 29:1527–1553.
Cho JR, Lee SY (2003). Dynamic analysis of baffled fuel-storage tanks using the ALE finite element method. Int. J. Numer. Methods Fluids 41:185–208.
Dodge FT (2000). The New Dynamic Behavior of Liquids in Moving Containers. Southwest Research Institute, San Antonio.
Ehrlich LW, Riley JD, Strange WG, Troesch BA (1961). Finite difference techniques for a boundary problem with an eigenvalue in a boundary condition. J. Appl. Math. J. Sot. Ind. 9:149-164.
Gedikli A, Erguven ME (1999). Seismic analysis of a liquid storage tank with a baffle. J. Sound Vib. 223(1):141–155.
Ibrahim RA (2005). Liquid Sloshing Dynamics, Theory and Applications. Cambridge University Press, New York.
Lee SY, Cho JR (2002). Baffled fuel-storage container: Parametric study on transient dynamic characteristics. J. Struct. Eng. Mech. 13(6):653–670.
Lomen DO (1965). Liquid propellant sloshing in mobile tanks of arbitrary shapes.NASA-CR-222.
Modi VJ, Akinturk A (2002). An efficient liquid sloshing damper for control of wind-induced instabilities. J. Wind Eng. Ind. Aerodyn. 90:1907–1918.
Pal NC, Bhattacharyya SK, Sinha PK (2002). Non-linear coupled slosh dynamics of liquid-filled laminated composite containers: A two dimensional finite element approach. J. Sound Vib. 261(1):729–749.
Qing Li, Xingrui M, Tianshu W (2011). Equivalent mechanical model for liquid sloshing during draining. J. Acta Astronautica. 68:91–100.
Wang ZL, Liu YZ (2002). Fluid-filled System Dynamics. Science Press, Beijing, in Chinese.
Welt F, Modi VJ (1992). Vibration damping through liquid sloshing, Part I: A nonlinear analysis. J. Vib. Acoust. 114:10–16.
Xu L, Dai L (2003). A mechanical model for dynamic behavior of large amplitude liquid sloshing in partially filled tank vehicles. Proceedings of IMECE'03. ASME International Mechanical Engineering Congress. Washington DC.